Deficits in the activity of presynaptic γ-aminobutyric acid type B receptors contribute to altered neuronal excitability in fragile X syndrome

Received for publication, December 17, 2016, and in revised form, February 7, 2017 Published, Papers in Press, February 17, 2017, DOI 10.1074/jbc.M116.772541

Ji-Yong Kang[‡], Jayashree Chadchankar[‡], Thuy N. Vien[‡], Michelle I. Mighdoll[§], Thomas M. Hyde[§¶], Robert J. Mather[‡‖], Tarek Z. Deeb[‡], Menelas N. Pangalos[**], Nicholas J. Brandon[‡‖], John Dunlop[‡‖], and Stephen J. Moss[‡‖‡‡1]

From the [‡]AstraZeneca Tufts Laboratory for Basic and Translational Neuroscience, Tufts University School of Medicine, Boston, Massachusetts 02111, the [§]Lieber Institute for Brain Development and [¶]Departments of Neurology and Psychiatry and Behavioral Sciences, The Johns Hopkins University School of Medicine, Baltimore, Maryland 21205, [‖]Neuroscience, Innovative Medicines and Early Development, AstraZeneca, Waltham, Massachusetts 02451, [**]Innovative Medicines and Early Development, AstraZeneca, Melbourn Science Park, Cambridge Road, Royston Herts SG8 6EE, United Kingdom, and the [‡‡]Department of Neuroscience, Physiology and Pharmacology, University College, London WC1E 6BT, United Kingdom

Edited by F. Anne Stephenson

The behavioral and anatomical deficits seen in fragile X syndrome (FXS) are widely believed to result from imbalances in the relative strengths of excitatory and inhibitory neurotransmission. Although modified neuronal excitability is thought to be of significance, the contribution that alterations in GABAergic inhibition play in the pathophysiology of FXS are ill defined. Slow sustained neuronal inhibition is mediated by γ-aminobutyric acid type B ($GABA_B$) receptors, which are heterodimeric G-protein-coupled receptors constructed from R1a and R2 or R1b and R2 subunits. Via the activation of $G_{i/o}$, they limit cAMP accumulation, diminish neurotransmitter release, and induce neuronal hyperpolarization. Here we reveal that selective deficits in R1a subunit expression are seen in Fmr1 knock-out mice (KO) mice, a widely used animal model of FXS, but the levels of the respective mRNAs were unaffected. Similar trends of R1a expression were seen in a subset of FXS patients. $GABA_B$ receptors ($GABA_B$Rs) exert powerful pre- and postsynaptic inhibitory effects on neurotransmission. R1a-containing $GABA_B$Rs are believed to mediate presynaptic inhibition in principal neurons. In accordance with this result, deficits in the ability of $GABA_B$Rs to suppress glutamate release were seen in Fmr1-KO mice. In contrast, the ability of $GABA_B$Rs to suppress GABA release and induce postsynaptic hyperpolarization was unaffected. Significantly, this deficit contributes to the pathophysiology of FXS as the $GABA_B$R agonist (*R*)-baclofen rescued the imbalances between excitatory and inhibitory neurotransmission evident in Fmr1-KO mice. Collectively, our results provided evidence that selective deficits in the activity of presynaptic $GABA_B$Rs contribute to the pathophysiology of FXS.

Fragile X syndrome (FXS)[2] is the most common cause of inherited intellectual disability and the leading monogenic cause of autism spectrum disorders. Approximately one in every 4,000 males and one in every 6,000 females are diagnosed with FXS, and the patients suffer from developmental, cognitive, and neuropsychological complications throughout life (1, 2). FXS originates from the silencing of the fragile X mental retardation 1 (*FMR1*) gene, caused by hypermethylation of the expanded CGG trinucleotide repeats in the 5′-untranslated region (UTR) of the gene (3–6). *FMR1* codes for fragile X mental retardation protein (FMRP), an RNA-binding protein essential in regulating protein translation and synaptic plasticity (7–12). FMRP binds to numerous mRNAs important in neuronal network physiology, including calcium/calmodulin-dependent protein kinase type II α chain, amyloid precursor protein, postsynaptic density protein 95 (DLG4), γ-aminobutyric acid receptor subunits δ and β-1, and myelin basic protein (13).

Our understanding of the pathophysiology FXS has been greatly facilitated by the development of a mouse model that lacks expression of the FMR1 protein (Fmr1-KO) (14, 15). Fmr1-KO mice share several phenotypes with FXS patients such as altered spine morphology, cognitive deficits, hyperactivity, sensory hypersensitivity, repetitive behaviors, and macroorchidism (15, 16). Studies from Fmr1-KO mice have revealed profound alterations in excitatory neurotransmission that are thought to primarily arise from excessive activity of

This work was supported by National Institutes of Health NINDS Grants NS051195, NS056359, NS081735, R21NS080064, and NS087662 and NIMH Grant MH097446 and United States Department of Defense Grant AR140209 (to S. J. M.). S. J. M. serves as a consultant for AstraZeneca and SAGE Therapeutics, relationships that are regulated by Tufts University and do not impact this study. At the time this work was conducted, R. J. M., M. N. P., N. J. B., and J. D. were full-time employees and shareholders in AstraZeneca. The content is solely the responsibility of the authors and does not necessarily represent the official views of the National Institutes of Health.

[1] To whom correspondence should be addressed: Dept. of Neuroscience, Tufts University School of Medicine, Boston, MA 02111. Tel.: 617-636-3976; Fax: 617-636-2413; E-mail: Stephen.Moss@Tufts.edu.

[2] The abbreviations used are: FXS, fragile X syndrome; *FMR1*, fragile X mental retardation 1; FMRP, fragile X mental retardation protein; mGluR, metabotropic glutamate receptor; E/I, excitatory/inhibitory; $GABA_B$R, $GABA_B$ receptor; GIRK, G-protein-activated inwardly rectifying potassium; eEPSC, evoked excitatory postsynaptic current; PPF, paired pulse facilitation; eIPSC, evoked inhibitory synaptic current; (*R*)-Bac, (*R*)-baclofen; sEPSC, spontaneous EPSC; sIPSC, spontaneous IPSC; TUBB, β-tubulin; ACSF, artificial cerebral spinal fluid; PBST, PBS with Tween 20.

group 1 metabotropic glutamate receptors (mGluR1/5) (17). Increased mGluR1/5 signaling is believed to enhance the removal of α-amino-3-hydroxy-5-methyl-4-isoxazolepropionic acid (AMPA) receptors from excitatory synapses. This process leads to exaggerated long term depression, a well studied model of synaptic plasticity, which is believed to contribute to the deficits in dendritic morphology seen in FXS (9).

In addition to compromised glutamatergic neurotransmission, deficits in the efficacy of inhibitory neurotransmission are also implicated in FXS, leading to the concept that imbalances in the efficacy of excitatory and inhibitory neurotransmission (E/I balance) drive the behavioral and anatomical deficits (18–22). Slow prolonged synaptic inhibition in the brain is mediated by GABA$_B$Rs, which are heterodimeric G-protein-coupled receptors composed of GABA$_B$R1 and GABA$_B$R2 subunits that activate $G_{i/o}$ signaling pathways. Their activation leads to diminished neurotransmitter release and increased neuronal hyperpolarization (23–25). Two major isoforms of GABA$_B$R1 are found in mammals, R1a and R1b (26). R1a-containing GABA$_B$ receptors are enriched predominantly in axonal terminals of glutamatergic neurons, whereas postsynaptic GABA$_B$Rs contain R1b subunits (27–31). There has been considerable interest in the use of the selective GABA$_B$R agonist baclofen as a treatment for FXS (32–36). However, it remains to be determined whether deficits in GABA$_B$R signaling directly contribute to the pathophysiology of FXS.

In this study, we have compared GABA$_B$R expression levels and function in the hippocampus of Fmr1-KO mice. We demonstrate selective down-regulation of the GABA$_B$R1a isoform in Fmr1-KO mice and post-mortem hippocampi from FXS patients. This deficit compromised the ability of (*R*)-baclofen to reduce excitatory neurotransmission without compromising its ability to modify GABAergic neurotransmission. Furthermore, (*R*)-baclofen was able to alleviate the deficits in E/I balance seen in Fmr1-KO mice. Collectively, our results provide a rationale why correcting deficits in GABA$_B$R signaling may be a useful therapeutic strategy in FXS.

Results

Inactivation of the Fmr1 gene in mice leads to selective deficits in GABA$_B$R1 subunit expression

To address whether alterations in GABA$_B$ receptor signaling contribute to the pathophysiology of FXS, we used Fmr1-KO mice maintained on a C57BL/6 background (14). We first assessed GABA$_B$ receptor expression levels in the hippocampus of male Fmr1-KO and age-matched male wild-type (WT) controls (Fig. 1, *A* and *B*) using immunoblotting. In SDS-soluble extracts, an antibody specific to GABA$_B$R1 (University of California Davis/National Institutes of Health NeuroMab, N94A/49) detected two bands, R1a and R1b, respectively.

As detailed previously, the R1a isoform is slightly larger (108 kDa) than R1b isoform (95 kDa) due to the presence of additional N-terminal extracellular sushi domains (27). Expression levels of the R1a subunit were significantly decreased in Fmr1-KO mice (5 weeks old) (Fig. 1, *A* and *B*; WT = 0.78 ± 0.15 and Fmr1-KO = 0.24 ± 0.02, *t* test, $p = 0.02$, $n = 3$). However, expression of R1b was comparable between genotypes (WT = 0.87 ± 0.12 and Fmr1-KO = 0.91 ± 0.09, *t* test, $p = 0.77$, $n = 3$) as was expression of the GABA$_B$R2 subunit (WT = 3.21 ± 0.16 and Fmr1-KO = 3.31 ± 0.40, $p = 0.83$, $n = 3$). Significantly, deficits in R1a expression were seen in the cortex and midbrain (Fig. 1, *C–F*; cortex, $p < 0.01$; midbrain, $p < 0.01$; *t* test, $n = 3–4$). To further evaluate the mechanism underlying the deficits in GABA$_B$R1 expression seen in Fmr1-KO, we assessed possible effects on the levels of the encoding mRNAs using quantitative PCR. This revealed that the levels of the R1a, R1b, and R2 subunit mRNAs were comparable in WT and Fmr1-KO mice (Fig. 2*A*).

The efficacy of GABA$_B$R signaling is subject to dynamic modulation via direct phosphorylation of serine residues 783 and 892 in the R2 subunit (37). Immunoblotting with the respective phosphospecific antibodies revealed that phosphorylation of both residues was comparable between WT and Fmr1-KO mice (Fig. 3, *A* and *B*).

As a means of further analyzing GABA$_B$R expression in Fmr1-KO mice, hippocampal sections were stained with a GABA$_B$R1 antibody, as specified, and imaged by confocal microscopy. Within CA1 (WT = 69.4 ± 12.2 and Fmr1-KO = 41.6 ± 2.7, *t* test, $p < 0.01$, $n = 18–21$ cells) and the dentate gyrus (WT = 65.5 ± 9.1 and Fmr1-KO = 39.3 ± 1.6, *t* test, $p < 0.01$, $n = 52–70$ cells) decreases in the maximum expression level of the GABA$_B$R1 subunit were seen in Fmr1-KO mice, consistent with the phenotype identified by immunoblotting (Fig. 3, *C–F*). Thus, Fmr1-KO mice exhibit selective deficits in GABA$_B$R1a expression compared with WT mice.

Deficits in GABA$_B$R expression are evident in post-mortem tissue from FXS patients

To examine the translational significance of our measurements in mice, we compared the expression levels of GABA$_B$Rs in posterior hippocampal tissue from three FXS patients and three controls (Fig. 3; male, Caucasian, and 72–86 years old). Two FXS patients showed weak expression of R1a isoform but comparable R1b isoform expression relative to control individuals (Fig. 4*A*, *red square*). One FXS patient did not show any change in R1a or R1b expression. GABA$_B$R2 subunit expression was similar across the subjects (Fig. 4*B*). Quantitative PCR revealed that levels of the R1a, R1b, and R2 subunit mRNAs were unaltered in FXS patients (Fig. 2*B*). The respective patient demographics are shown in Fig. 4*D*. Given the limited availability of post-mortem tissue, our results suggest that, in common with Fmr-1-KO mice, a similar trend of decreased GABA$_B$R1 subunit is seen in a subset of FXS patients.

GABA$_B$R-dependent modulation of excitatory transmission is reduced in Fmr1-KO mice

GABA$_B$Rs exert profound pre- and postsynaptic effects on neuronal excitability via the activation of $G_{i/o}$. More specifically, they reduce neurotransmitter release via inhibiting voltage-gated Ca^{2+} channels, whereas postsynaptically they induce hyperpolarization via the activation of G-protein-activated inwardly rectifying potassium (GIRK) channels (24, 25).

To assess whether Fmr1-KO mice exhibit impaired GABA$_B$R signaling, we first examined their ability to modulate glutamatergic neurotransmission. To do so, we examined the effects of

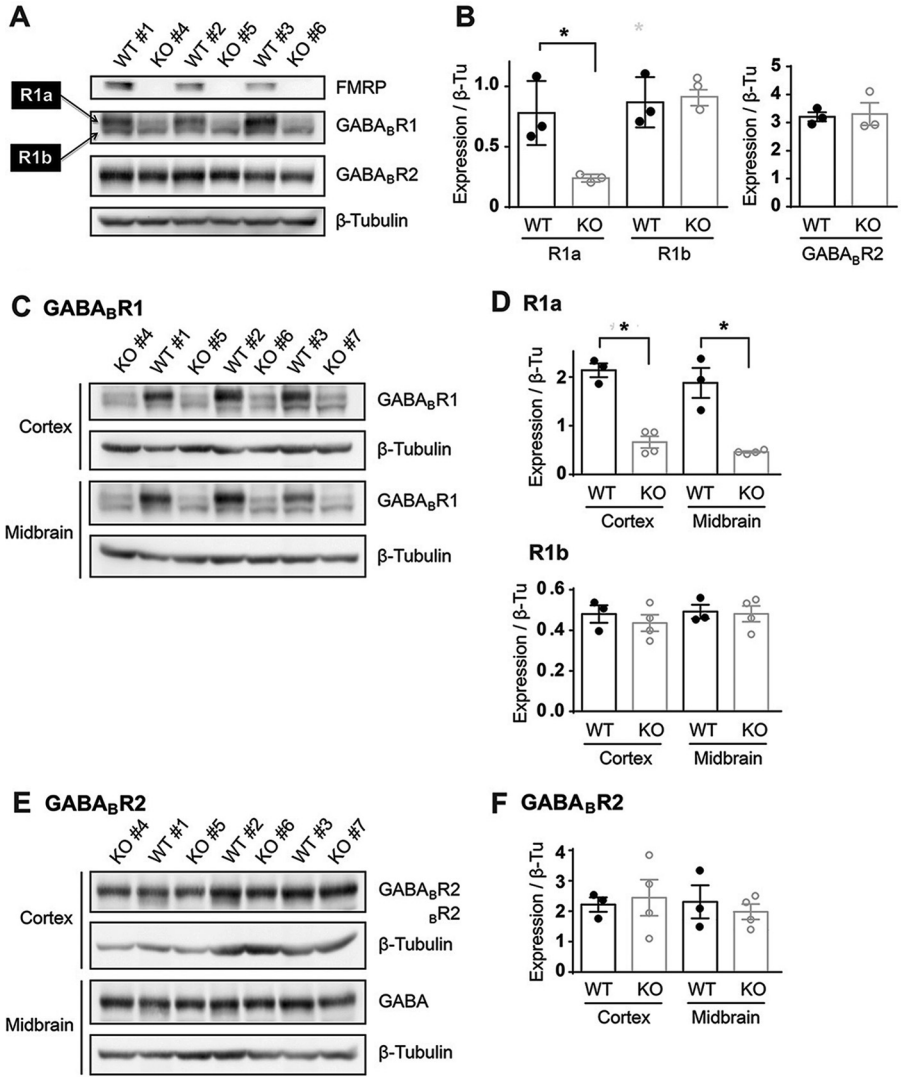

Figure 1. Analyzing GABA$_B$R Expression in Fmr1-KO and WT mice. *A*, representative Western blots of FMRP, GABA$_B$R1, GABA$_B$R2, and β-tubulin (5 weeks old, male, hippocampus). FMRP is not expressed in Fmr1-KO mice. GABA$_B$R1 subunit is shown as a doublet composed of R1a (*upper* band, *arrow*) and R1b (*lower* band, *arrow*). R1a was selectively decreased in Fmr1-KO mice. Neither R1b nor GABA$_B$R2 expression was different between Fmr1-KO and WT mice. *B*, quantification of GABA$_B$ receptor expression normalized to β-tubulin expression (*β-Tu*). Fmr1-KO mice, $n = 3$; WT mice, $n = 3$; *t* test, *, $p = 0.025$. *C*, representative results from Western blotting of GABA$_B$R1 and β-tubulin in prefrontal cortex and midbrain (9 weeks old, male). R1a down-regulation is observed in Fmr1-KO mice in different brain regions. *D*, quantification of R1a and R1b expression normalized to β-tubulin. Fmr1-KO mice, $n = 4$; WT mice, $n = 3$; *t* test; cortex *, $p < 0.01$; midbrain *, $p < 0.01$. *E*, Western blot of GABA$_B$R2 and β-tubulin in prefrontal cortex and midbrain (from the same animals as *C*) *F*, quantification of GABA$_B$R2 expression normalized to β-tubulin. Fmr1-KO mice, $n = 4$; WT mice, $n = 3$. *Error bars* represent S.E.

the GABA$_A$R agonist (*R*)-baclofen on the properties of evoked excitatory postsynaptic currents (eEPSCs) in the CA1 region of the hippocampus following activation of the Schaffer collateral pathway (Fig. 5*A*). Consistent with published studies, (*R*)-baclofen decreased eEPSC amplitude in WT mice (Fig. 5*B*). Interestingly, in Fmr-1KO mice, 5 μM (*R*)-baclofen was less effective in suppressing eEPSCs (Fig. 5*C*) as the residual current observed in the presence of this drug was significantly higher than that seen in WT (Fig. 5*D*; WT = 0.13 ± 0.01 and Fmr1-KO = 0.27 ± 0.04, *t* test, $p < 0.01$, $n = 3$ animals per group, 11–31 recordings from each animal). To control for the specificity of the effects seen with (*R*)-baclofen, we assessed whether the ability of adenosine A1 receptors to modulate eEPSCs was altered in Fmr1-KO mice. In common with GABA$_B$Rs, A1 receptors modulate eEPSCs via activation of $G_{i/o}$ (38, 39). In contrast to (*R*)-baclofen, the effects of adenosine on eEPSCs were comparable between genotypes (Fig. 5*D*).

To further analyze the role of GABA$_B$Rs in regulating excitatory neurotransmission, paired pulse facilitation (PPF) was compared between Fmr1-KO and WT mice (Fig. 5, *E–G*). PPF was defined as follows: (Amplitude of the second peak − Amplitude of the first peak)/Amplitude of the first peak. Importantly, Fmr1-KO mice showed higher PPF than WT mice before baclofen administration (*t* test, $p < 0.01$, $n = 5–8$ slices). Consistent with previous results (40, 41), (*R*)-baclofen potentiated PPF in WT mice (Fig. 5*E*; before = 1.06 ± 0.11 and (*R*)-Bac = 1.42 ± 0.17, *t* test, $p < 0.01$, $n = 5$ slices). However, in Fmr1-KO mice, baclofen did not modulate PPF (Fig. 5*F*; before = 1.41 ± 0.12 and (*R*)-Bac = 1.36 ± 0.14, *t* test, $p = 0.79$, $n = 8$ slices). Expressed as a percentage of

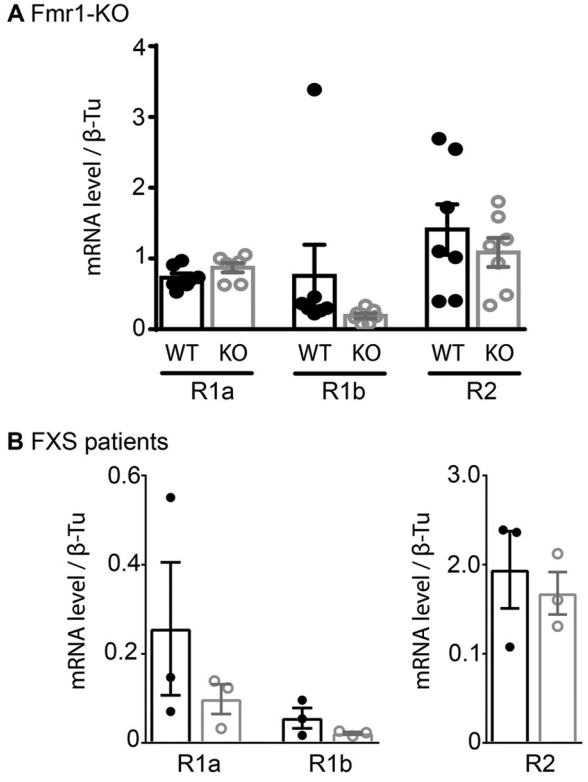

Figure 2. Comparing the levels of GABA$_B$R1a, GABA$_B$R1b, and GABA$_B$R2 mRNAs in the hippocampus of Frm1-KO and FXS patients. cDNA was prepared from the hippocampi of Frm1-KO mice (*A*) and FXS patients (*B*) and subjected to quantitative PCR. Expression is calculated relative to β-tubulin (*β-Tu*) mRNA levels. Frm1-KO mice, *open circles*, $n = 7$; wild-type mice, *solid circles*, $n = 7$; FXS patients, *open circles*, $n = 4$; control, *solid circles*, $n = 3$. *Error bars* represent S.E.

change, PPF modulation by baclofen in WT synapses was significantly greater than in Fmr1-KO synapses, further indicating a deficit in GABA$_B$R signaling (Fig. 5*G*; WT = 37.6 ± 16.0% and Fmr1-KO = −3.4 ± 9.8%; *t* test; *, $p = 0.02$; $n = 5–8$ slices).

Collectively, our results suggest that the ability of GABA$_B$Rs to modulate excitatory neurotransmission is compromised in Fmr1-KO mice, which correlates with reduced R1a subunit expression as shown in Fig. 1. Consistent with our results, R1a-deficient mice show selective deficits in the ability of GABA$_B$Rs to modulate excitatory neurotransmission (27, 28).

The ability of GABA$_B$Rs to modulate inhibitory neurotransmission is comparable in WT and Fmr1-KO mice

To assess whether Fmr1-KO mice exhibit global deficits in GABA$_B$R signaling, we compared the ability of baclofen to modulate inhibitory neurotransmission between genotypes. First we compared the ability of presynaptic GABA$_B$Rs to modulate inhibitory neurotransmission between strains. To do so, we compared the effects of baclofen and adenosine to regulate the evoked inhibitory synaptic currents (eIPSCs) in CA1 neurons following activation of the Schaffer collateral pathway. The ability of baclofen and adenosine to modulate eIPSCs was comparable between genotypes (Fig. 6, *A–C*; WT (*R*)-Bac = 0.36 ± 0.07 and Fmr1-KO (*R*)-Bac = 0.38 ± 0.09, *t* test, $p = 0.82$, $n = 6–7$ slices). Next we analyzed the efficacy of postsynaptic GABA$_B$R signaling by comparing the ability of (*R*)-baclofen to activate GIRK channels. (*R*)-Baclofen exerted similar effects in WT and Fmr1-KO mice (Fig. 6, *D* and *E*; WT = 3.35 ± 0.57 pA/picofarad and Fmr1-KO = 3.31 ± 0.59 pA/picofarad, *t* test, $p = 0.96$, $n = 5$ slices). Thus, in contrast to our observations on excitatory neurotransmission, the ability of GABA$_B$R to modulate inhibitory synaptic transmission was unaltered in Fmr1-KO mice.

Comparing the properties of spontaneous EPSCs and IPSCs and their modulation by baclofen in Fmr-1-KO mice

To ascertain the significance of our findings with GABA$_B$Rs for the pathophysiology of FXS, we compared the properties of spontaneous excitatory and inhibitory synaptic currents in CA1 neurons from WT and Fmr1-KO mice using voltage clamp recordings (Fig. 7). Spontaneous EPSCs (sEPSCs) were recorded at −70 mV in the presence of 50 μM picrotoxin, whereas spontaneous inhibitory postsynaptic currents (sIPSCs) were measured at the same potential in the presence of 50 μM 2-amino-5-phosphonopentanoic acid and 10 μM 6,7-dinitroquinoxaline-2,3-dione. sEPSC frequency was significantly lower in Fmr1-KO mice (Fig. 7*A*; WT = 6.69 ± 0.11 Hz and Fmr1-KO = 6.04 ± 0.10 Hz, Dunn's post hoc test, $p < 0.01$, $n = 12–14$ cells). This decrease in sEPSC frequency is consistent with the reductions in presynaptic GABA$_B$R-dependent modulation of eEPSCs and increased PPF seen in Fmr1-KO mice (Fig. 4). In addition to this, Fmr1-KO mice exhibited lower sIPSC frequency (Fig. 7*B*; WT = 10.66 ± 0.07 Hz and Fmr1-KO = 9.05 ± 0.07 Hz, Dunn's post hoc test, $p < 0.01$, $n = 18–19$ cells), leading to a net increase in the ratio of sEPSC/sIPSC frequency (Fig. 7*C*; WT = 0.63 ± 0.01 and Fmr1-KO = 0.67 ± 0.01, Dunn's post hoc test, $p < 0.01$, $n = 12–14$ cells). The deficit in sEPSC/sIPSC frequency in Fmr1-KO mice was "normalized" to levels seen in WT mice upon exposure to a subsaturating concentration of 5 μM (*R*)-baclofen (Fig. 7*C*; WT = 0.23 ± 0.02 and Fmr1-KO = 0.25 ± 0.03, Dunn's post hoc test, $p > 0.99$, $n = 12–14$ cells).

We also compared sEPSC and sIPSC amplitudes between genotypes. Fmr1-KO mice exhibited larger sEPSC amplitudes (Fig. 7*A*; WT = 19.65 ± 0.29 and Fmr1-KO = 20.26 ± 0.31, Dunn's post hoc test, $p < 0.01$, $n = 12–14$ cells). However, sIPSC amplitudes were reduced in Fmr1-KO mice (Fig. 7*B*; WT = 63.48 ± 0.53 and Fmr1-KO = 40.14 ± 0.91, Dunn's post hoc test, $p < 0.01$, $n = 18–19$ cells), leading to an increase in the ratio of sEPSC/sIPSC amplitude (Fig. 6*D*; WT = 0.31 ± 0.00 and Fmr1-KO = 0.50 ± 0.01, Dunn's post hoc test, $p < 0.01$, $n = 12–14$ cells). This modification in sIPSC amplitude is likely to arise from alterations in the activity of GABA$_A$Rs that have been previously observed in Fmr-1 KO mice (42). Consistent with this, (*R*)-baclofen was unable to fully reverse the alterations in sEPSC/sIPSC amplitude seen in Fmr1-KO mice (Fig. 7*D*; WT = 0.39 ± 0.02 and Fmr1-KO = 0.44 ± 0.02, Dunn's post hoc test, $p < 0.01$ $n = 12–14$ cells).

Finally, the relative charge transfer of spontaneous activity was determined by multiplying peak event area by frequency (43). The ratio of sEPSC/sIPSC charge transfer or "E/I balance" was then compared between genotypes (Fig. 7*E*). Changes in both frequency and amplitude contributed to a net increase of E/I balance charge transfer in Fmr1-KO mice (Fig. 7*E*; WT =

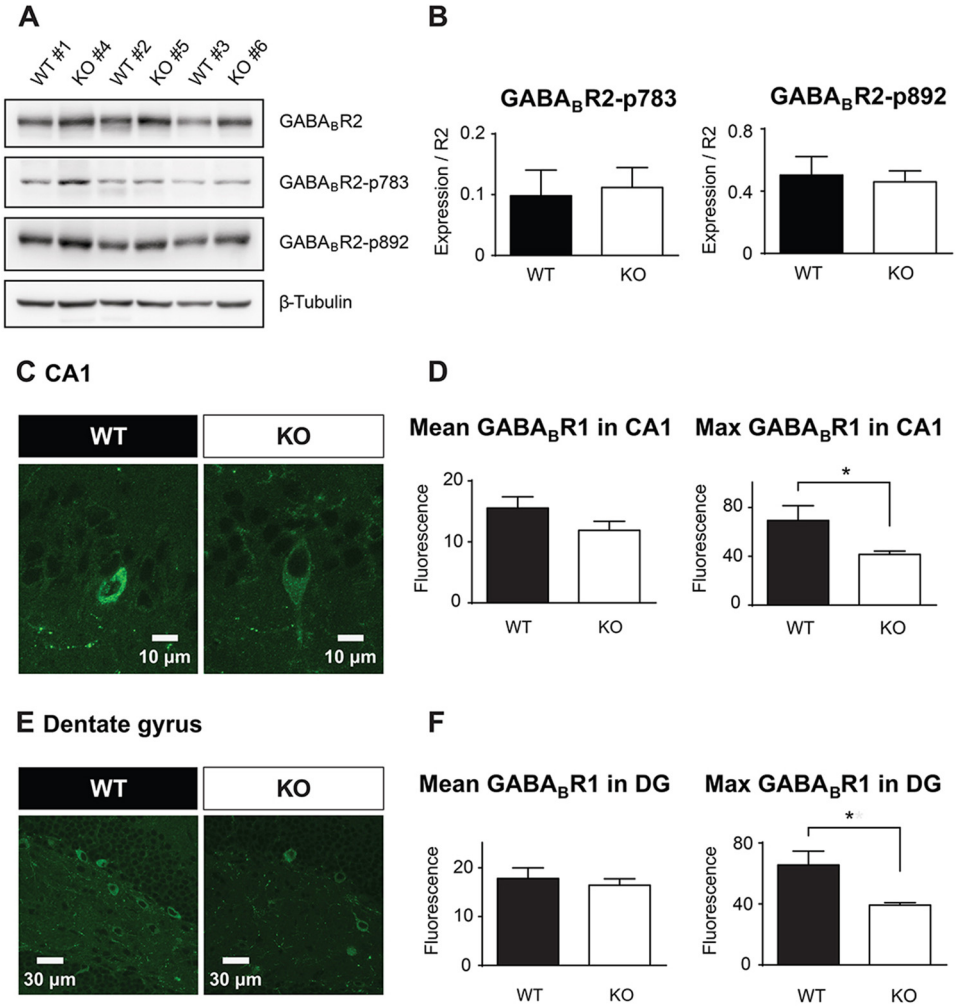

Figure 3. Analyzing GABA$_B$R phosphorylation in Fmr1-KO and WT mice. Western blots of phosphorylated GABA$_B$R2 from Fmr1-KO and WT mice whole-cell brain lysates are shown. *A*, representative Western blot of the total GABA$_B$R2, GABA$_B$R2-Ser(P)-783, GABA$_B$R2-Ser(P)-892, and β-tubulin (5 weeks old, male, hippocampus). *B*, quantification of phosphorylation relative to the total GABA$_B$R2 expression (*R2*). Fmr1-KO mice, *open bars*, $n = 3$; WT mice, *solid bars*, $n = 3$. *C–F*, immunohistochemical staining of acute hippocampal slice CA1 (*C* and *D*) and dentate gyrus (*E* and *F*) regions from Fmr1-KO and WT mice (5 weeks old, male). *C*, representative fluorescence image of hippocampal CA1 region stained with GABA$_B$R1 antibody. *D*, quantified fluorescence levels from GABA$_B$R1-positive neurons in CA1 region ($n = 18–21$ cells from six mice) showed slightly decreased mean GABA$_B$R1 staining (*left*) and significantly lower maximum GABA$_B$R1 staining (*right*) in Fmr1-KO mice. Fmr1-KO mice, *open bars*; WT mice, *solid bars*; *t* test; *, $p < 0.01$. *E*, representative fluorescence image of hippocampal dentate gyrus region stained with GABA$_B$R1 antibody. *F*, quantified fluorescence levels from GABA$_B$R1-positive neurons in dentate gyrus ($n = 52–70$ cells from six mice) showed slightly decreased mean GABA$_B$R1 staining (*left*) and significantly lower maximum GABA$_B$R1 staining (*right*) in Fmr1-KO mice. Fmr1-KO mice, *open bars*; WT mice, *solid bars*; *t* test; *, $p < 0.01$. *Error bars* represent S.E.

0.22 ± 0.01 and Fmr1-KO $= 0.29 \pm 0.01$, Dunn's post hoc test, $p < 0.01$, $n = 12–14$ cells). Significantly, this imbalance was normalized in Fmr1-KO mice by exposure to (*R*)-baclofen (Fig. 7*E*; WT $= 0.11 \pm 0.01$ and Fmr1-KO $= 0.10 \pm 0.02$, Dunn's post hoc test, $p = 0.36$, $n = 12–14$ cells). Collectively, these results reveal that Fmr1-KO mice have deficits in the properties of sEPSC and sIPSC that result in a net relative increase of excitatory/inhibitory transmission, a phenomenon that can be reversed by the GABA$_B$R agonist (*R*)-baclofen.

Discussion

In this study, we compared GABA$_B$R expression levels and signaling in the brains of Fmr1-KO mice. In this model of FXS, we establish that GABA$_B$R1a subunit protein expression was significantly decreased in multiple brain regions. In contrast, the expression levels of GABA$_B$R1b and GABA$_B$R2 subunits were comparable between genotypes. Significantly, the levels of the mRNAs encoding GABA$_B$Rs were comparable in Fmr1-KO mice with those in WT, suggesting that FMRP does not act to modify the stability and or transcription of the respective gene transcripts. Interestingly, similar trends in GABA$_B$R1 expression were seen in a small sample of post-mortem brain samples obtained from male FXS patients. However, the paucity of suitable human tissue precluded further investigation of these observations.

Evidence accrued from isoform-specific knock-out mice strongly suggests that the sushi domains at the N terminus of GABA$_B$R1a subunits are critical in determining the accumulation of heterodimeric GABA$_B$Rs on presynaptic glutamatergic terminals. GABA$_B$Rs on these structures are believed to play a key role in limiting glutamate release and in modulating synaptic plasticity. In keeping with our biochemical deficits, the ability of (*R*)-baclofen to suppress eEPSCs was decreased in Fmr1-KO mice. Likewise, a selective deficit in PPF was

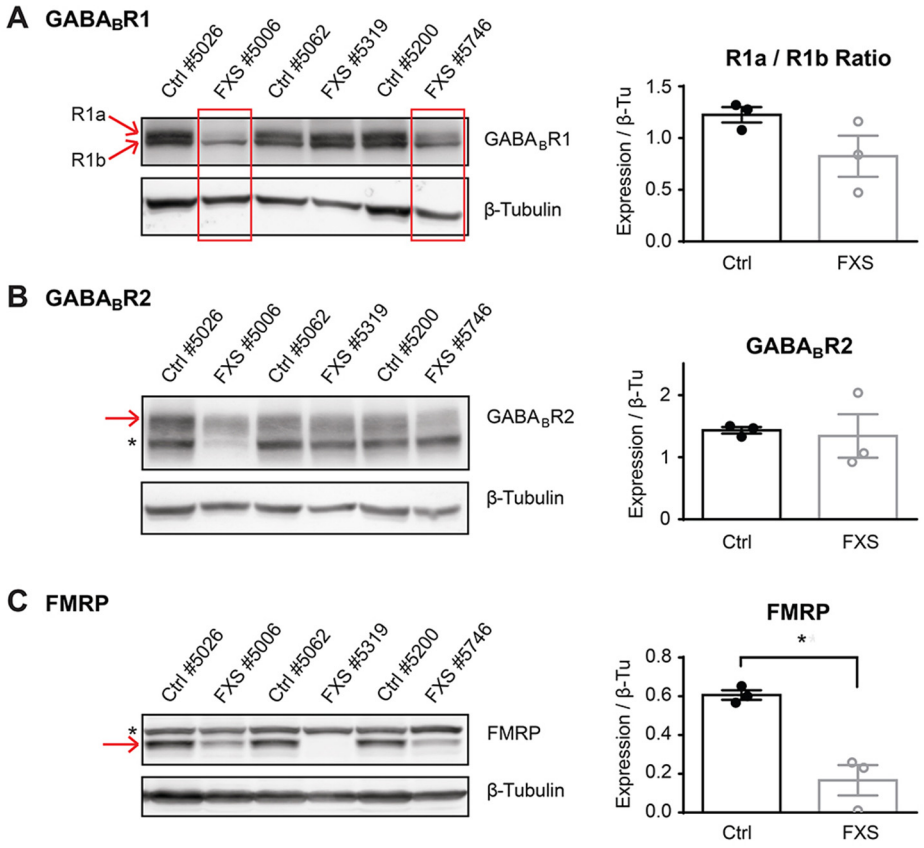

D Patient demographics

#	DISORDER	AGE	SEX	RACE	PMI (hrs)	pH	CAUSE OF DEATH
5026	Control	86.07	M	C	22	n/a	multiple injuries
5062	Control	82.66	M	C	25.5	n/a	blunt force head trauma
5200	Control	71.91	M	C	14.5	n/a	HACD
5006	FXS	86	M	C	5	6.38	complications of disorder
5319	FXS	72	M	C	17	6.99	complications of disorder
5746	FXS	80	M	C	22	n/a	complications of disorder

Abbreviations: PMI (post mortem interval), M (male), C (Caucasian), n/a (not available), HACD (Heavy Alpha Chain Disease), FXS (Fragile X Syndrome)

Figure 4. Comparing GABA$_B$R expression in the hippocampus of fragile X patients. *A*, *left*, GABA$_B$R1 Western blot. GABA$_B$R1 is shown as a doublet composed of R1a (*upper* band, *arrow*) and R1b (*lower* band, *arrow*). *Right*, quantification of R1a/R1b expression ratio relative to β-tubulin (*β-Tu*). Control (*Ctrl*) individuals, *black*, $n = 3$; FXS patients, *gray*, $n = 3$. *B*, Western blot of GABA$_B$R2 (*left*) and expression level quantified relative to β-tubulin (*right*). Control individuals, *black*, $n = 3$; FXS patients, *gray*, $n = 3$. The *asterisk* likely represents a truncated GABA$_B$R2 protein. *C*, Western blot of FMRP (*left*) and expression level quantified relative to β-tubulin (*right*). The *asterisk* represents a nonspecific band. Control individuals, *black*, $n = 3$; FXS patients, *gray*, $n = 3$; *t* test; **, $p < 0.01$. *D*, patient demographics of fragile X patients and control individuals. *Error bars* represent S.E.

observed in Fmr1-KO mice. These deficits are likely to arise from reduced levels of GABA$_B$R expression and not GPCR effector coupling as the ability of adenosine receptors to suppress EPSCs was not compromised in the Fmr1-KO mice. GABA$_B$Rs composed of R1b/R2 are found on GABAergic presynaptic specializations and postsynaptic sites adjacent to dendritic spines where they regulate GABA release and neuronal hyperpolarization, respectively. In agreement with our biochemical studies, the ability of GABA$_B$Rs to modulate eIPSCs and induce GIRK channel-mediated hyperpolarization was comparable in Fmr1-KO and WT mice. The frequency of spontaneous synaptic activity in Fmr1-KO mice did not change upon (*R*)-baclofen application, further demonstrating deficient GABA$_B$R modulation in axonal terminals. Thus, collectively, our results suggest that Fmr1-KO mice have selective deficits in the function of presynaptic GABA$_B$Rs on principal neurons. This in turns leads to a reduction in the ability of (*R*)-baclofen to regulate excitatory neurotransmission.

It is widely believed that alterations in E/I balance are central to the behavioral and anatomical deficits seen in FXS. Therefore, we examined whether the deficits in GABA$_B$R signaling seen in Fmr1-KO mice impact these respective parameters. Consistent with our biochemical and electrophysiological measurements, which suggest selective deficits in GABA$_B$R receptor signaling in glutamatergic nerve terminals, the deficits in E/I balance are reversed by (*R*)-baclofen. This highly stable and potent GABA$_B$R agonist may be more effective in activating the

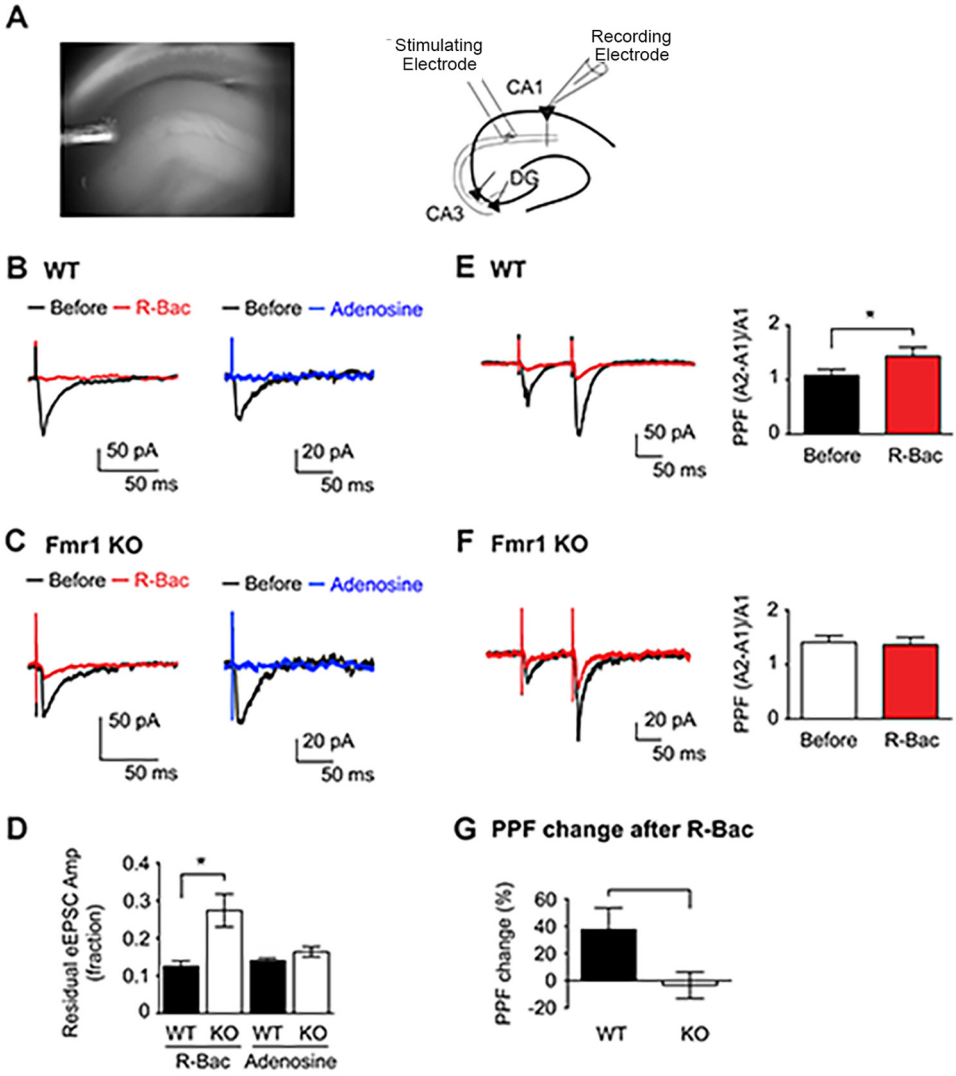

Figure 5. Analyzing the effects of GABA$_B$R activation on excitatory neurotransmission in Fmr1-KO and WT mice. *A*, an exemplary bright field image of acute slice (*top*) and schematic representation (*bottom*) of recording. The Shaffer collaterals were stimulated using a stimulating electrode, and effects on CA1 pyramidal cell activity were recorded by whole-cell patch clamp. eEPSCs were measured from the CA1 region after stimulating from Schaffer collateral (0.1-ms pulse, 0.5 Hz, −70 mV). *B*, exemplar traces of eEPSCs recorded from WT under control conditions before (*black*) and after exposure to 5 μM (*R*)-baclofen (*red*) or 100 μM adenosine. *C*, exemplar traces of eEPSCs recorded from Fmr1-KO under control conditions before (*black*) and after exposure to 5 μM (*R*)-baclofen (*red*) or 100 μM adenosine. *D*, amplitude of residual eEPSCs after 5 μM (*R*)-baclofen or 100 μM adenosine. Fmr1-KO mice, *open bars*, $n = 5$ mice; WT mice, *solid bars*, $n = 5$ mice; 11–31 eEPSCs were measured from each animal and averaged; *t* test; *, $p < 0.01$. *E–G*, PPF of eEPSCs was measured from the CA1 region after stimulating from Schaffer collateral (0.1-ms pulse, 100-ms interval, 0.33 Hz, −70 mV). *E*, representative WT eEPSC traces (*left*) and quantification (*right*) showing PPF before (*black*) and after (*red*) 1 μM (*R*)-baclofen ($n = 65$ from five animals; *, $p < 0.01$). *F*, *left*, representative Fmr1-KO eEPSC traces showing PPF before (*black*) and after (*red*) 1 μM (*R*)-baclofen. *Right*, quantification of PPF before (*white*) and after (*red*) 1 μM (*R*)-baclofen ($n = 8$ mice). *G*, PPF change after 1 μM (*R*)-baclofen from WT (*solid bars*, $n = 5$ animals) and Fmr1-KO (*open bars*, $n = 8$ mice) (*t* test; *, $p = 0.02$). *Error bars* represent S.E. *DG*, dentate gyrus.

remaining populations of GABA$_B$Rs in Fmr1-KO compared with the endogenous neurotransmitter GABA. Consistent with this notion, there is evidence that GABA levels are also diminished in FXS (1–4, 20). Collectively, these results suggest that the deficits in R1a subunit expression levels and subsequent signaling seen in our experiments contribute to altered neuronal excitability seen in FXS. In keeping with this view, it is interesting to note that R1a knock-out mice share some phenotypes in common with Fmr1-KO mice. In particular, both strains exhibit cognitive deficits, social avoidance, and sleep disturbance (27, 44–49). Thus, some of the phenotypes seen in FXS are likely to arise from deficits in the activity of GABA$_B$Rs containing R1a subunits.

The mechanisms by which FMRP impacts GABA$_B$R function remain to be determined. However, our results strongly suggest that FMRP does not modulate the expression levels of the mRNAs encoding these receptors. A study using a cross-linking-immunoprecipitation assay revealed that FMRP binds to GABA$_B$R1 and GABA$_B$R2 in the mouse brain; however, this result has been difficult to reproduce in subsequent studies (13, 50). It is also emerging that GABA$_B$R activity itself may play a role in promoting FMRP expression in neurons (51). FMRP is enriched in the soma and dendrites via its interaction with the messenger ribonucleoprotein complex (10). Less is understood about the role FMRP plays in axonal terminals; however, it is implicated in axon guidance and pre-

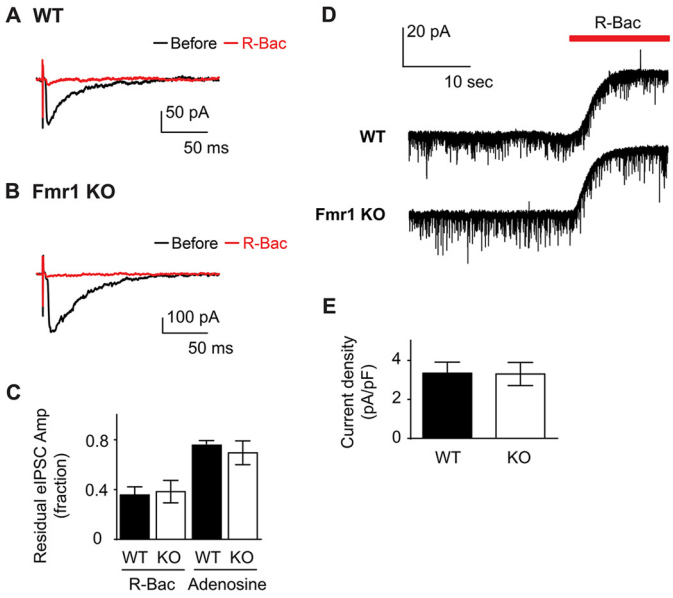

Figure 6. Comparing the effects of GABA$_B$R activation on inhibitory neurotransmission in Fmr1-KO and WT mice. *A–C*, eIPSCs were measured from the CA1 region after stimulating from the Schaffer collateral (0.1-ms pulse, 0.5 Hz, −70 mV). *A*, WT. *B*, Fmr1-KO. Representative eIPSC traces before (*black*) and after (*red*) 10 μM (*R*)-baclofen application are shown. *C*, amplitude (*Amp*) of residual eIPSCs after 10 μM (*R*)-baclofen or 100 μM adenosine. Fmr1-KO mice, *open bars*, $n = 6$ mice; WT mice, *solid bars*, $n = 6$ mice; 2–14 eIPSC were measured from each animal and averaged. *D–F*, sIPSCs were measured from the CA1 region. (*R*)-Baclofen perfusion activated GIRK current. *D*, representative sIPSC traces from WT (*black*) and Fmr1-KO (*green*) mice. 10 μM (*R*)-baclofen was applied in the bath as indicated (*red bar*). *E*, GIRK current density is plotted. Fmr1-KO mice, *open bars*, $n = 5$ mice; WT mice, *solid bars*, $n = 5$ mice. *Error bars* represent S.E. *pF*, picofarad.

synaptic short term plasticity (10, 52–54). It has been estimated that upward of 30% of the presynaptic proteome is potentially regulated by FMRP (55). However, it is unclear which of these potential binding partners influence the function of presynaptic GABA$_B$Rs in glutamatergic nerve terminals. It may be possible that FMRP binds directly to GABA$_B$Rs to regulate their functions as similar modulation of big potassium (BK) channels by FMRP has recently been reported in CA3 pyramidal neurons (56).

In summary, our results highlight the importance of GABA$_B$R dysfunction in FXS. Further investigation of the mechanism by which GABA$_B$Rs are modulated or controlled by FMRP could aid the development of improved therapeutic strategies that target GABA$_B$Rs for the treatment of FXS.

Experimental procedures

Animals

Fmr1-KO mice were originally purchased from The Jackson Laboratory (B6.129P2-Fmr1tm1Cgr/J) and then bred in house (homozygous female × hemizygous male). Fmr1-KO and WT C57BL/6 mice were housed under constant temperature and humidity on a 12-h light/dark cycle with standard rodent food and water *ad libitum*. Male mice were used in the current study. All animal protocols were carried out in accordance with the National Institutes of Health Guide for the Care and Use of Laboratory Animals and were approved by Institutional Animal Care and Use Committee of Tufts University.

Antibodies

The following antibodies were used for Western blotting: anti-GABA$_B$R1 (for mouse; 1:1000; University of California Davis/National Institutes of Health NeuroMab, N94A/49), anti-GABA$_B$R1 (for human; 1:1000; Millipore, AB2256), anti-GABA$_B$R2 (1:1000; University of California Davis/National Institutes of Health NeuroMab, N81/2), anti-β-tubulin (1:10,000; Millipore, 05661), anti-FMRP (1:1000; Abcam, ab17722), anti-phospho-Ser-783-GABA$_B$R2 (1:1000; PhosphoSolutions, p1148-783) (57), and anti-phospho-Ser-892-GABA$_B$R2 (Ser(P)-S892) (The Rockefeller University, Protein/DNA Technology Center) (58). The following antibody was used for immunohistochemistry: anti-GABA$_B$R1 (for human; 1:1000; Millipore, AB2256).

Human tissue

Post-mortem hippocampal brain tissues from FXS patients and control subjects were gifted from the Lieber Institute for Brain Development (Baltimore, MD). For the control subjects, consent for the use of post-mortem human brains was obtained through the Lieber Institute for Brain Development under Maryland Department of Health and Mental Hygiene protocol number 12-24 and Western Institutional Review Board protocol number 20111080. Clinical characterization, macroscopic and microscopic neuropathological examinations, toxicological analyses, and quality control measures were performed as described previously (59, 60). Each subject was diagnosed retrospectively by two board-certified psychiatrists according to criteria in the Diagnostic and Statistical Manual of Mental Disorders, 4th Ed. A psychiatric narrative summary was compiled for every case from a combination of data from a telephone screening on the day of donation with next of kin; from police, autopsy, and toxicology reports; from psychiatric records; from family informant interviews with next of kin (a psychological autopsy interview and the Structured Clinical Interview for Diagnostic and Statistical Manual of Mental Disorders, 4th Ed.); and from interviews with psychiatric treatment providers (59). The healthy controls had no known history of psychiatric illness or substance abuse or dependence and were screened for drug intoxication at time of death. The information about neuroleptic and antidepressant medications in subjects with psychiatric disorders was acquired from toxicology testing as described previously (60). The FXS tissue was obtained by the National Institute of Child Health and the Human Development Brain and Tissue Bank for Developmental Disorders under contracts NO1-HD-4-3368 and NO1-HD-4-3383. The Institutional Review Board of the University of Maryland at Baltimore and the State of Maryland approved the protocol. The University of Maryland cases were processed, curated, handled, and evaluated in a similar fashion to the Lieber Institute for Brain Development cases. Brain specimens from the University of Maryland were transferred from University of Maryland to the Lieber Institute for Brain Development under a Materials Transfer Agreement.

Immunohistochemistry

Five-week-old male mice were intracardially perfused with 4% (w/v) paraformaldehyde. Brains were extracted and

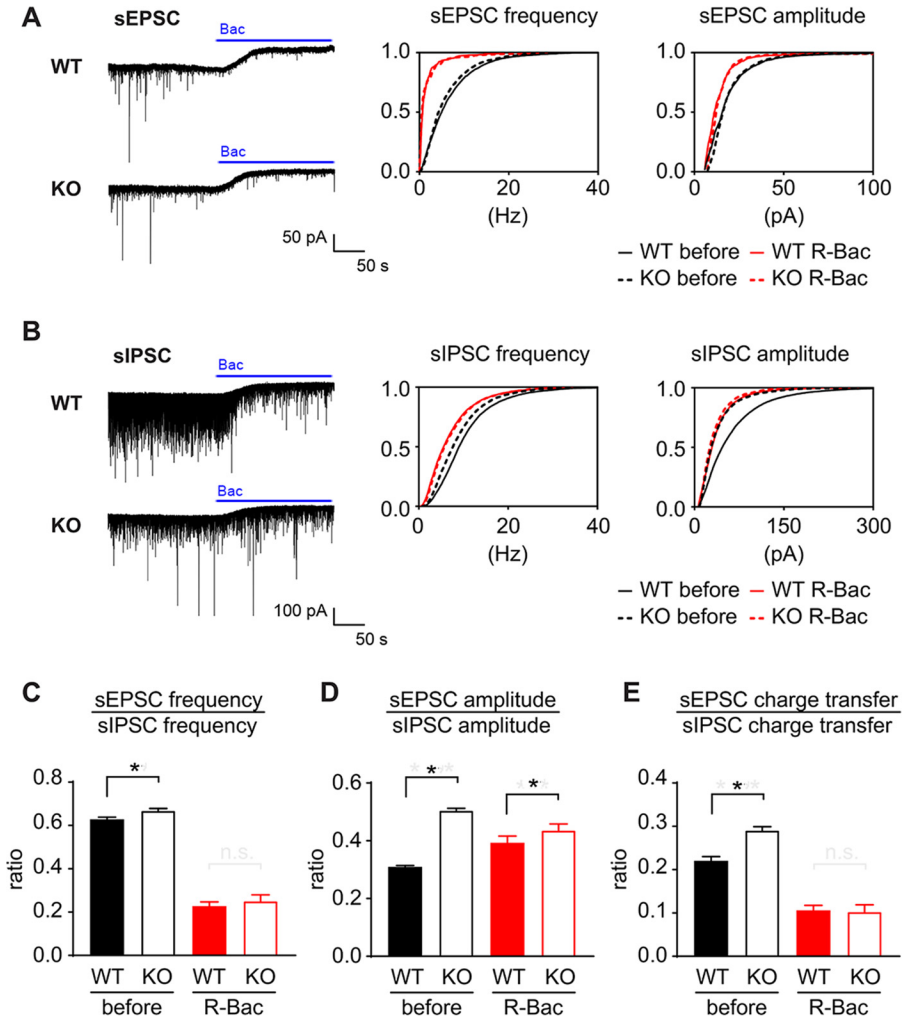

Figure 7. Analyzing the efficacies of excitatory and inhibitory neurotransmission in Fmr1-KO and WT mice. Whole-cell recordings from the CA1 region of acute hippocampal slices of WT and Fmr1-KO mice (5 weeks old, male) are shown. Spontaneous EPSCs and IPSCs were recorded from a single cell held at −70 mV. *A*, *left*, representative traces of sEPSCs from WT and KO mice. *Middle*, histograms of sEPSC frequency are plotted for WT (*solid line*) and Fmr1-KO (*dashed line*) mice before (*black*) and after (*red*) 5 μM baclofen was perfused in the bath. Before (*R*)-baclofen, Dunn's post hoc test, $p < 0.01$; after (*R*)-baclofen, Dunn's post hoc test, $p > 0.99$. *Right*, histograms of sEPSC amplitude are plotted for WT (*solid line*) and Fmr1-KO (*dashed line*) mice before (*black*) and after (*red*) 5 μM baclofen was perfused in the bath. Before (*R*)-baclofen, Dunn's post hoc test, $p < 0.01$; after (*R*)-baclofen, Dunn's post hoc test, $p = 0.7338$. *B*, *left*, representative traces of sIPSCs from WT and KO mice. *Middle*, histograms of sIPSC frequency are plotted for WT (*solid line*) and Fmr1-KO (*dashed line*) mice before (*black*) and after (*red*) 5 μM baclofen was perfused in the bath. Before (*R*)-baclofen, Dunn's post hoc test, $p < 0.01$; after (*R*)-baclofen, Dunn's post hoc test, $p = 0.10$. *Right*, histogram of sIPSC amplitude is plotted for WT (*solid line*) and Fmr1-KO (*dashed line*) mice before (*black*) and after (*red*) 5 μM baclofen was perfused in the bath. Before (*R*)-baclofen, Dunn's post hoc test, $p < 0.01$; after (*R*)-baclofen, Dunn's post hoc test, $p < 0.01$. *C*, ratio of sEPSC frequency over sIPSC frequency is plotted. Before (*R*)-baclofen, Dunn's post hoc test; *, $p < 0.01$; after (*R*)-baclofen, Dunn's post hoc test, $p > 0.99$. *D*, ratio of sEPSC amplitude over sIPSC amplitude is plotted. Before (*R*)-baclofen, Dunn's post hoc test; *, $p < 0.01$; after (*R*)-baclofen, Dunn's post hoc test; *, $p < 0.01$. *E*, ratio of sEPSC synaptic transmission over sIPSC transmission is plotted. Before (*R*)-baclofen, Dunn's post hoc test; *, $p < 0.01$; after (*R*)-baclofen, Dunn's post hoc test, $p = 0.3571$. *Error bars* represent S.E.

immersed in 30% (w/v) sucrose for 72 h. Coronal sections of 40-μm thickness were prepared, and free-floating sections were rinsed in BupH-PBS (Thermo Fisher Scientific), blocked for 1 h in 10% (w/v) BSA with 0.3% Triton X-100 in PBS, and incubated overnight at room temperature with the indicated antibodies. The following day, the tissue was rinsed in PBS and incubated for 2 h in Alexa Fluor 488 secondary antibodies (Life Technologies, Thermo Fisher Scientific). After extensive rinsing with PBS, tissues were mounted, dried, and placed on coverslips with ProLong Gold antifade reagent (Invitrogen). Images were acquired with a Nikon Ti microscope and analyzed using NIH ImageJ. Images were recorded using the same microscope settings for each treatment and were taken within the linear range as detailed previously (61). Controls were obtained by incubating slices in the absence of primary antibody. Data were presented as mean ± S.E.

Quantitative PCR

RNA was extracted from mouse and human hippocampi using the RNeasy Lipid Tissue Mini kit (Qiagen). cDNA was synthesized using a SuperScript® III First-Strand Synthesis kit (Life Technologies) with random hexamers following the manufacturer's instructions. For quantitative PCR, cDNA was amplified using 600 nM primers and 2× SYBR Green Master Mix in a volume of 25 μl in the Mx3000P system (Agilent) in duplicates using the following primers: mouse: GABA$_B$R1a: forward, 5′-CCTGCCTGTGGACTATGAGATTG; reverse, 5′-CAGATGGAAGTCGGGGTCAC; GABA$_B$R1b: forward,

5′-CTCTTCTGCTGGTGATGGC; reverse, 5′-TACTGCACGCCGTTCTGAG; GABA$_B$R2: forward, 5′-GACCTGCGACTCTACGACACC; reverse, 5′-GCGTTGTCTGAGGGCACC; TUBB: forward, 5′-GAGGATCAATGTCTACTACAATGAGGC; reverse, 5′-CCTCTCGGATCTTGCTGATGAG; human: GABA$_B$R1a: forward, 5′-AGATCATACACCCGCCCTG; reverse, 5′-ACCTTCCCATTTTCCAGGGT; GABA$_B$R1b: forward, 5′-CTGCCGCTTCTGGTTGTGA; reverse, 5′-CCGTTCTGAGGAGGGGTGC; GABA$_B$R2: forward, 5′-CGACCTGCGGCTCTATGAC; reverse, 5′-GGCTGGATTCACCGCATTG; TUBB: forward, 5′-CAGAGCGGTGCTGGTGGAC; reverse, 5′-GAGGGCACCACGCTGAAG. The gene dose was calculated based on the standard curve method relative to *TUBB* and normalized to mean control values.

Slice electrophysiology

Five-week-old male Fmr1-KO or WT mice were decapitated under isoflurane anesthesia. The brain was dissected and coronal hippocampal slices (310 μm) were prepared in an ice-cold solution containing 87 mM NaCl, 3 mM KCl, 7 mM $MgCl_2$, 0.5 mM $CaCl_2$, 1.25 mM NaH_2PO_4, 50 mM sucrose, 25 mM glucose, and 25 mM $NaHCO_3$ continuously bubbled with 95% and 5% O_2/CO_2 carbogen. Slices were warmed to 33–34 °C and incubated for 45 min in carbogen-bubbled artificial cerebral spinal fluid (ACSF) (126 mM NaCl, 2.5 mM KCl, 2 mM $MgCl_2$, 2 mM $CaCl_2$, 1.25 mM NaH_2PO_4, 1 mM L-glutamine, 1.5 mM sodium pyruvate, 10 mM glucose, and 26 mM $NaHCO_3$) supplemented with 3 mM *myo*-inositol and 0.4 mM ascorbic acid. For whole-cell recordings, a coronal slice was transferred to the recording chamber and superfused with ACSF at 30 °C. Neurons were visualized with a digital camera (Andor) on a fixed stage upright microscope (Nikon FN-PT) with a 40× water immersion objective equipped with differential interference contrast/infrared optics. Whole-cell patch clamp recordings were made from pyramidal neurons in the CA1 region of dorsal hippocampus using an Axopatch 200B amplifier (Molecular Devices) and a Digidata 1550 digitizer (Molecular Devices).

For eEPSCs and eIPSCs, a stimulating electrode (FHC, model CBARC75) was positioned to stimulate Schaffer collaterals and commanded by a Stimulus Isolator (World Precision Instruments). Patch pipettes were filled with internal solution (140 mM KCl, 2 mM $MgCl_2$, 0.1 mM $CaCl_2$, 1.1 mM EGTA, 10 mM HEPES, 2 mM MgATP, 1 mM NaGTP, and 10 mM sodium phosphocreatine, pH 7.4). Series resistance and whole-cell capacitance were continually monitored throughout the experiments. Using voltage clamp, eEPSCs and eIPSCs were recorded at −70 mV in response to electrical stimulation. For sEPSC and eEPSC recordings, ACSF supplemented with 50 μM picrotoxin was perfused for 2–3 min before recording. For sIPSC and eIPSC recordings, ACSF supplemented with 50 μM 2-amino-5-phosphonopentanoic acid and 20 μM 6,7-dinitroquinoxaline-2,3-dione was perfused for 2–3 min before recording. Recordings were analyzed in pClamp 10.5 (Clampfit, Axon Instruments). Recording data were also analyzed using MiniAnalysis software (Synaptosoft, Inc.). Data were presented as mean ± S.E.

Western blotting

Hippocampal, prefrontal cortical, and midbrain tissues were dissected from isoflurane-anesthetized Fmr1-KO and WT mice (3–16 weeks), flash frozen, and stored at −80 °C. Alternatively, post-mortem hippocampal tissues from FXS and control subjects were used. On the day of experiment, the brain tissue was homogenized in lysis buffer containing 20 mM Tris-HCl, pH 8.0, 150 mM NaCl, 1% Triton X-100, 0.1% SDS, 5 mM EDTA, 10 mM NaF, 2 mM Na_3VO_4, and 10 mM sodium pyrophosphate plus 1:1000 protease inhibitors 4-(2-aminoethyl)benzenesulfonyl fluoride, antipain, aprotinin, leupeptin, and pepstatin. After incubating for an hour at 4 °C, the brain lysate was centrifuged at 13,200 rpm at 4 °C for 15 min. Using standard Western blotting techniques, the supernatant was subjected to SDS-PAGE (8–10% gel) and transferred to a nitrocellulose membrane overnight at 4 °C. The membrane was blocked with 5% nonfat milk in PBST for an hour. Subsequently, it was incubated in a specific primary antibody in 5% milk in PBST. After rigorous washes, a specific horseradish peroxidase-conjugated secondary antibody (in 5% milk in PBST) was incubated with the membrane for an hour at room temperature. The blots were developed using enhanced chemiluminescence systems (Amresco and Thermo Fisher Scientific), imaged using the charge-coupled device-based LAS 3000 system (FujiFilm), and quantified with NIH ImageJ software. Data were presented as mean ± S.E.

Author contributions—J.-Y. K., T. N. V., J. C., M. I. M., and T. M. H. conducted the experiments, analyzed the results, and co-wrote paper. R. J. M., M. N. P., J. D., N. J. B., T. Z. D., and S. J. M. conceived and coordinated the study. S. J. M., N. J. B., and T. Z. D. wrote the paper with J.-Y. K. All authors analyzed the results and approved the final version of the manuscript.

References

1. Chiurazzi, P., Neri, G., and Oostra, B. A. (2003) Understanding the biological underpinnings of fragile X syndrome. *Curr. Opin. Pediatr.* **15,** 559–566
2. Garber, K. B., Visootsak, J., and Warren, S. T. (2008) Fragile X syndrome. *Eur. J. Hum. Genet.* **16,** 666–672
3. Pieretti, M., Zhang, F. P., Fu, Y. H., Warren, S. T., Oostra, B. A., Caskey, C. T., and Nelson, D. L. (1991) Absence of expression of the FMR-1 gene in fragile X syndrome. *Cell* **66,** 817–822
4. Devys, D., Lutz, Y., Rouyer, N., Bellocq, J. P., and Mandel, J. L. (1993) The FMR-1 protein is cytoplasmic, most abundant in neurons and appears normal in carriers of a fragile X premutation. *Nat. Genet.* **4,** 335–340
5. O'Donnell, W. T., and Warren, S. T. (2002) A decade of molecular studies of fragile X syndrome. *Annu. Rev. Neurosci.* **25,** 315–338
6. Kooy, R. F. (2003) Of mice and the fragile X syndrome. *Trends Genet.* **19,** 148–154
7. Ashley, C. T., Jr., Wilkinson, K. D., Reines, D., and Warren, S. T. (1993) FMR1 protein: conserved RNP family domains and selective RNA binding. *Science* **262,** 563–566
8. Siomi, H., Siomi, M. C., Nussbaum, R. L., and Dreyfuss, G. (1993) The protein product of the fragile X gene, FMR1, has characteristics of an RNA-binding protein. *Cell* **74,** 291–298
9. Huber, K. M., Gallagher, S. M., Warren, S. T., and Bear, M. F. (2002) Altered synaptic plasticity in a mouse model of fragile X mental retardation. *Proc. Natl. Acad. Sci. U.S.A.* **99,** 7746–7750
10. Jin, P., and Warren, S. T. (2003) New insights into fragile X syndrome: from molecules to neurobehaviors. *Trends Biochem. Sci.* **28,** 152–158

11. Antar, L. N., and Bassell, G. J. (2003) Sunrise at the synapse: the FMRP mRNP shaping the synaptic interface. *Neuron* **37,** 555–558
12. Maurin, T., Zongaro, S., and Bardoni, B. (2014) Fragile X syndrome: from molecular pathology to therapy. *Neurosci. Biobehav. Rev.* **46,** 242–255
13. Pasciuto, E., and Bagni, C. (2014) SnapShot: FMRP mRNA targets and diseases. *Cell* **158,** 1446–1446.e1
14. Bakker, C. E., Verheij, C., Willemsen, R., van der Helmm, R., Oerlemans, F., Vermey, M., Bygrave, A., Hoogeveen, A., Oostra, B. A., Reyniers, E., De Boule, K., D'Hooge, R., Cras, P., van Velzen, D., Nagels, G., *et al.* (1994) Fmr1 knockout mice: a model to study fragile X mental retardation. The Dutch-Belgian Fragile X Consortium. *Cell* **78,** 23–33
15. Bakker, C. E., and Oostra, B. A. (2003) Understanding fragile X syndrome: insights from animal models. *Cytogenet. Genome Res.* **100,** 111–123
16. Rotschafer, S. E., and Razak, K. A. (2014) Auditory processing in fragile X syndrome. *Front. Cell. Neurosci.* **8,** 19
17. Bear, M. F., Huber, K. M., and Warren, S. T. (2004) The mGluR theory of fragile X mental retardation. *Trends Neurosci.* **27,** 370–377
18. D'Hulst, C., and Kooy, R. F. (2007) The GABA$_A$ receptor: a novel target for treatment of fragile X? *Trends Neurosci.* **30,** 425–431
19. Chang, S., Bray, S. M., Li, Z., Zarnescu, D. C., He, C., Jin, P., and Warren, S. T. (2008) Identification of small molecules rescuing fragile X syndrome phenotypes in *Drosophila*. *Nat. Chem. Biol.* **4,** 256–263
20. Curia, G., Papouin, T., Séguéla, P., and Avoli, M. (2009) Downregulation of tonic GABAergic inhibition in a mouse model of fragile X syndrome. *Cereb. Cortex.* **19,** 1515–1520
21. D'Hulst, C., Heulens, I., Brouwer, J. R., Willemsen, R., De Geest, N., Reeve, S. P., De Deyn, P. P., Hassan, B. A., and Kooy, R. F. (2009) Expression of the GABAergic system in animal models for fragile X syndrome and fragile X associated tremor/ataxia syndrome (FXTAS). *Brain Res.* **1253,** 176–183
22. Cea-Del Rio, C. A., and Huntsman, M. M. (2014) The contribution of inhibitory interneurons to circuit dysfunction in fragile X syndrome. *Front. Cell. Neurosci.* **8,** 245
23. Couve, A., Moss, S. J., and Pangalos, M. N. (2000) GABA$_B$ receptors: a new paradigm in G protein signaling. *Mol. Cell. Neurosci.* **16,** 296–312
24. Gassmann, M., and Bettler, B. (2012) Regulation of neuronal GABA$_B$ receptor functions by subunit composition. *Nat. Rev. Neurosci.* **13,** 380–394
25. Benke, D., Balakrishnan, K., and Zemoura, K. (2015) Regulation of cell surface GABA$_B$ receptors: contribution to synaptic plasticity in neurological diseases. *Adv. Pharmacol.* **73,** 41–70
26. Kaupmann, K., Huggel, K., Heid, J., Flor, P. J., Bischoff, S., Mickel, S. J., McMaster, G., Angst, C., Bittiger, H., Froestl, W., and Bettler, B. (1997) Expression cloning of GABA$_B$ receptors uncovers similarity to metabotropic glutamate receptors. *Nature* **386,** 239–246
27. Vigot, R., Barbieri, S., Bräuner-Osborne, H., Turecek, R., Shigemoto, R., Zhang, Y. P., Luján, R., Jacobson, L. H., Biermann, B., Fritschy, J. M., Vacher, C. M., Müller, M., Sansig, G., Guetg, N., Cryan, J. F., *et al.* (2006) Differential compartmentalization and distinct functions of GABA$_B$ receptor variants. *Neuron* **50,** 589–601
28. Ulrich, D., and Bettler, B. (2007) GABA$_B$ receptors: synaptic functions and mechanisms of diversity. *Curr. Opin. Neurobiol.* **17,** 298–303
29. Biermann, B., Ivankova-Susankova, K., Bradaia, A., Abdel Aziz, S., Besseyrias, V., Kapfhammer, J. P., Missler, M., Gassmann, M., and Bettler, B. (2010) The Sushi domains of GABA$_B$ receptors function as axonal targeting signals. *J. Neurosci.* **30,** 1385–1394
30. Hannan, S., Wilkins, M. E., and Smart, T. G. (2012) Sushi domains confer distinct trafficking profiles on GABA$_B$ receptors. *Proc. Natl. Acad. Sci. U.S.A.* **109,** 12171–12176
31. Hannan, S., Gerrow, K., Triller, A., and Smart, T. G. (2016) Phospho-dependent accumulation of GABA$_B$Rs at presynaptic terminals after NMDAR activation. *Cell Rep.* **16,** 1962–1973
32. Pacey, L. K., Heximer, S. P., and Hampson, D. R. (2009) Increased GABA$_B$ receptor-mediated signaling reduces the susceptibility of fragile X knockout mice to audiogenic seizures. *Mol. Pharmacol.* **76,** 18–24
33. Pacey, L. K., Tharmalingam, S., and Hampson, D. R. (2011) Subchronic administration and combination metabotropic glutamate and GABA$_B$ receptor drug therapy in fragile X syndrome. *J. Pharmacol. Exp. Ther.* **338,** 897–905
34. Henderson, C., Wijetunge, L., Kinoshita, M. N., Shumway, M., Hammond, R. S., Postma, F. R., Brynczka, C., Rush, R., Thomas, A., Paylor, R., Warren, S. T., Vanderklish, P. W., Kind, P. C., Carpenter, R. L., Bear, M. F., *et al.* (2012) Reversal of disease-related pathologies in the fragile X mouse model by selective activation of GABA$_B$ receptors with arbaclofen. *Sci. Transl. Med.* **4,** 152ra128
35. Erickson, C. A., Veenstra-Vanderweele, J. M., Melmed, R. D., McCracken, J. T., Ginsberg, L. D., Sikich, L., Scahill, L., Cherubini, M., Zarevics, P., Walton-Bowen, K., Carpenter, R. L., Bear, M. F., Wang, P. P., and King, B. H. (2014) STX209 (arbaclofen) for autism spectrum disorders: an 8-week open-label study. *J. Autism Dev. Disord.* **44,** 958–964
36. Schaefer, T. L., Davenport, M. H., and Erickson, C. A. (2015) Emerging pharmacologic treatment options for fragile X syndrome. *Appl. Clin. Genet.* **8,** 75–93
37. Terunuma, M., Vargas, K. J., Wilkins, M. E., Ramírez, O. A., Jaureguiberry-Bravo, M., Pangalos, M. N., Smart, T. G., Moss, S. J., and Couve, A. (2010) Prolonged activation of NMDA receptors promotes dephosphorylation and alters postendocytic sorting of GABA$_B$ receptors. *Proc. Natl. Acad. Sci. U.S.A.* **107,** 13918–13923
38. Thompson, S. M., Haas, H. L., and Gähwiler, B. H. (1992) Comparison of the actions of adenosine at pre- and postsynaptic receptors in the rat hippocampus *in vitro*. *J. Physiol.* **451,** 347–363
39. Schuler, V., Lüscher, C., Blanchet, C., Klix, N., Sansig, G., Klebs, K., Schmutz, M., Heid, J., Gentry, C., Urban, L., Fox, A., Spooren, W., Jaton, A. L., Vigouret, J., Pozza, M., *et al.* (2001) Epilepsy, hyperalgesia, impaired memory, and loss of pre- and postsynaptic GABA$_B$ responses in mice lacking GABA$_{B(1)}$. *Neuron* **31,** 47–58
40. Skov, J., Andreasen, M., Hablitz, J. J., and Nedergaard, S. (2011) Baclofen and adenosine inhibition of synaptic transmission at CA3-CA1 synapses display differential sensitivity to K^+ channel blockade. *Cell. Mol. Neurobiol.* **31,** 587–596
41. Porter, J. T., and Nieves, D. (2004) Presynaptic GABA$_B$ receptors modulate thalamic excitation of inhibitory and excitatory neurons in the mouse barrel cortex. *J. Neurophysiol.* **92,** 2762–2770
42. Braat, S., and Kooy, R. F. (2015) The GABA$_A$ receptor as a therapeutic target for neurodevelopmental disorders. *Neuron* **86,** 1119–1130
43. Gao, X. P., Liu, Q. S., Liu, Q., and Wong-Riley, M. T. (2011) Excitatory-inhibitory imbalance in hypoglossal neurons during the critical period of postnatal development in the rat. *J. Physiol.* **589,** 1991–2006
44. Jacobson, L. H., Kelly, P. H., Bettler, B., Kaupmann, K., and Cryan, J. F. (2006) GABA$_{B(1)}$ receptor isoforms differentially mediate the acquisition and extinction of aversive taste memories. *J. Neurosci.* **26,** 8800–8803
45. Shaban, H., Humeau, Y., Herry, C., Cassasus, G., Shigemoto, R., Ciocchi, S., Barbieri, S., van der Putten, H., Kaupmann, K., Bettler, B., and Lüthi, A. (2006) Generalization of amygdala LTP and conditioned fear in the absence of presynaptic inhibition. *Nat. Neurosci.* **9,** 1028–1035
46. Cullen, P. K., Dulka, B. N., Ortiz, S., Riccio, D. C., and Jasnow, A. M. (2014) GABA-mediated presynaptic inhibition is required for precision of long-term memory. *Learn. Mem.* **21,** 180–184
47. Vienne, J., Bettler, B., Franken, P., and Tafti, M. (2010) Differential effects of GABA$_B$ receptor subtypes, γ-hydroxybutyric acid, and baclofen on EEG activity and sleep regulation. *J. Neurosci.* **30,** 14194–14204
48. Kronk, R., Bishop, E. E., Raspa, M., Bickel, J. O., Mandel, D. A., and Bailey, D. B., Jr. (2010) Prevalence, nature, and correlates of sleep problems among children with fragile X syndrome based on a large scale parent survey. *Sleep* **33,** 679–687
49. Kasten, C. R., and Boehm, S. L., 2nd. (2015) Identifying the role of pre-and postsynaptic GABA$_B$ receptors in behavior. *Neurosci. Biobehav. Rev.* **57,** 70–87
50. Darnell, J. C., Van Driesche, S. J., Zhang, C., Hung, K. Y., Mele, A., Fraser, C. E., Stone, E. F., Chen, C., Fak, J. J., Chi, S. W., Licatalosi, D. D., Richter, J. D., and Darnell, R. B. (2011) FMRP stalls ribosomal translocation on mRNAs linked to synaptic function and autism. *Cell* **146,** 247–261
51. Zhang, W., Xu, C., Tu, H., Wang, Y., Sun, Q., Hu, P., Hu, Y., Rondard, P., and Liu, J. (2015) GABA$_B$ receptor upregulates fragile X mental retardation protein expression in neurons. *Sci. Rep.* **5,** 10468

52. Hanson, J. E., and Madison, D. V. (2007) Presynaptic FMR1 genotype influences the degree of synaptic connectivity in a mosaic mouse model of fragile X syndrome. *J. Neurosci.* **27,** 4014–4018
53. Christie, S. B., Akins, M. R., Schwob, J. E., and Fallon, J. R. (2009) The FXG: a presynaptic fragile X granule expressed in a subset of developing brain circuits. *J. Neurosci.* **29,** 1514–1524
54. Deng, P. Y., Sojka, D., and Klyachko, V. A. (2011) Abnormal presynaptic short-term plasticity and information processing in a mouse model of fragile X syndrome. *J. Neurosci.* **31,** 10971–10982
55. Darnell, J. C., and Klann, E. (2013) The translation of translational control by FMRP: therapeutic targets for FXS. *Nat. Neurosci.* **16,** 1530–1536
56. Deng, P. Y., Rotman, Z., Blundon, J. A., Cho, Y., Cui, J., Cavalli, V., Zakharenko, S. S., and Klyachko, V. A. (2013) FMRP regulates neurotransmitter release and synaptic information transmission by modulating action potential duration via BK channels. *Neuron* **77,** 696–711
57. Kuramoto, N., Wilkins, M. E., Fairfax, B. P., Revilla-Sanchez, R., Terunuma, M., Tamaki, K., Iemata, M., Warren, N., Couve, A., Calver, A., Horvath, Z., Freeman, K., Carling, D., Huang, L., Gonzales, C., *et al.* (2007) Phospho-dependent functional modulation of GABA$_B$ receptors by the metabolic sensor AMP-dependent protein kinase. *Neuron* **53,** 233–247
58. Couve, A., Thomas, P., Calver, A. R., Hirst, W. D., Pangalos, M. N., Walsh, F. S., Smart, T. G., and Moss, S. J. (2002) Cyclic AMP-dependent protein kinase phosphorylation facilitates GABA$_B$ receptor-effector coupling. *Nat. Neurosci.* **5,** 415–424
59. Kunii, Y., Hyde, T. M., Ye, T., Li, C., Kolachana, B., Dickinson, D., Weinberger, D. R., Kleinman, J. E., and Lipska, B. K. (2014) Revisiting DARPP-32 in postmortem human brain: changes in schizophrenia and bipolar disorder and genetic associations with t-DARPP-32 expression. *Mol. Psychiatry* **19,** 192–199
60. Lipska, B. K., Deep-Soboslay, A., Weickert, C. S., Hyde, T. M., Martin, C. E., Herman, M. M., and Kleinman, J. E. (2006) Critical factors in gene expression in postmortem human brain: focus on studies in schizophrenia. *Biol. Psychiatry* **60,** 650–658
61. Jacob, T. C., Michels, G., Silayeva, L., Haydon, J., Succol, F., and Moss, S. J. (2012) Benzodiazepine treatment induces subtype-specific changes in GABA$_A$ receptor trafficking and decreases synaptic inhibition. *Proc. Natl. Acad. Sci. U.S.A.* **109,** 18595–18600